Research Article

The purified extract of steamed *Panax ginseng* protects cardiomyocyte from ischemic injury *via* caveolin-1 phosphorylation-mediating calcium influx

Hai-Xia Li [a, b], Yan Ma [a], Yu-Xiao Yan [a], Xin-Ke Zhai [a], Meng-Yu Xin [a], Tian Wang [a], Dong-Cao Xu [a], Yu-Tong Song [a], Chun-Dong Song [c, **], Cheng-Xue Pan [a, *]

[a] *School of Pharmaceutical Sciences, Zhengzhou University, 100 Kexue Avenue, Zhengzhou, Henan Province, China*
[b] *Key Laboratory of Targeting Therapy and Diagnosis for Critical Diseases, Zhengzhou, Henan Province, China*
[c] *The First Affiliated Hospital of Henan University of Traditional Chinese Medicine, 9 Renmin Road, Zhengzhou, Henan Province, China*

A B S T R A C T

Background: Caveolin-1, the scaffolding protein of cholesterol-rich invaginations, plays an important role in store-operated Ca^{2+} influx and its phosphorylation at Tyr14 (p-caveolin-1) is vital to mobilize protection against myocardial ischemia (MI) injury. SOCE, comprising STIM1, ORAI1 and TRPC1, contributes to intracellular Ca^{2+} ($[Ca^{2+}]_i$) accumulation in cardiomyocytes. The purified extract of steamed *Panax ginseng* (EPG) attenuated $[Ca^{2+}]_i$ overload against MI injury. Thus, the aim of this study was to investigate the possibility of EPG affecting p-caveolin-1 to further mediate SOCE/$[Ca^{2+}]_i$ against MI injury in neonatal rat cardiomyocytes and a rat model.
Methods: PP2, an inhibitor of p-caveolin-1, was used. Cell viability, $[Ca^{2+}]_i$ concentration were analyzed in cardiomyocytes. In rats, myocardial infarct size, pathological damages, apoptosis and cardiac fibrosis were evaluated, p-caveolin-1 and STIM1 were detected by immunofluorescence, and the levels of caveolin-1, STIM1, ORAI1 and TRPC1 were determined by RT-PCR and Western blot. And, release of LDH, cTnI and BNP was measured.
Results: EPG, ginsenosides accounting for 57.96%, suppressed release of LDH, cTnI and BNP, and protected cardiomyocytes by inhibiting Ca^{2+} influx. And, EPG significantly relieved myocardial infarct size, cardiac apoptosis, fibrosis, and ultrastructure abnormality. Moreover, EPG negatively regulated SOCE *via* increasing p-caveolin-1 protein, decreasing ORAI1 mRNA and protein levels of ORAI1, TRPC1 and STIM1. More importantly, inhibition of the p-caveolin-1 significantly suppressed all of the above cardioprotection of EPG.
Conclusions: Caveolin-1 phosphorylation is involved in the protective effects of EPG against MI injury *via* increasing p-caveolin-1 to negatively regulate SOCE/$[Ca^{2+}]_i$.
© 2023 The Korean Society of Ginseng. Publishing services by Elsevier B.V. This is an open access article under the CC BY-NC-ND license (http://creativecommons.org/licenses/by-nc-nd/4.0/).

1. Introduction

Myocardial ischemia (MI) leading to myocardial infarction and followed by cardiac fibrosis represent a life-threatening condition.

Abundant evidences have suggested that $[Ca^{2+}]_i$ overload might participate in the pathogenesis and progress of the MI injury [1]. The enhancing Ca^{2+} influx promoted apoptosis and the effect was suppressed by removal of extracellular free Ca^{2+} in ischemic cardiomyocytes [2], and decrease of Ca^{2+} overload attenuated hypoxia-induced apoptosis in primary cardiomyocyte [3]. Moreover, $[Ca^{2+}]_i$ overloading can lead to cardiomyocyte necrosis and a replacement fibrosis [4]. Therefore, Ca^{2+} homeostasis is of pivotal interest for the cardiomyocytes.

Store-operated Ca^{2+} entry (SOCE) is a ubiquitous Ca^{2+} influx mechanism [5]. The molecular components of SOCE include stromal interaction molecule1 (STIM1), Ca^{2+} release activated Ca^{2+}

channel protein 1 (ORAI1) and transient receptor potential canonical 1 (TRPC1) proteins [6,7]. SOCE is triggered in response to depletion of sarcoplasmic reticulum (SR) Ca^{2+} stores [7]. After Ca^{2+} depletion, STIM1, as Ca^{2+} sensor localized at the SR membrane, undergoes a complex conformational rearrangement and redistributes to SR-plasma membrane junctions, then, it directly interacts with and opens ORAI1 to refill SR with Ca^{2+} [8,9]. Evidence also has shown that STIM1 can couple with and activate TRPC1 to contribute to SOCE activity [7,10]. The role of SOCE in the regulation of Ca^{2+} homeostasis was obtained in cardiomyocytes from embryo to adult [6,11,12], and there is growing support for the contribution of SOCE to Ca^{2+} overload [5,11] and ischemia-reperfusion (I/R) injury, and SOCE inhibitors can alleviate cardiac injury following I/R [13].

Caveolae, cholesterol-rich lipid rafts invaginations, orchestrate signaling in the cardiomyocytes [14]. Caveolin-1, the scaffolding protein of caveolae, provide protection for myocardium in ischemia injury [15]. Caveolin-1 phosphorylation (Tyr14) is essential for myocardial ischemic preconditioning (IPC) to mobilize endogenous protection [16]. Also, researches have shown that caveolin-1 can regulate store-operated Ca^{2+} influx [17]. In addition, caveolin-1 expression plays an anti-apoptotic role in H9c2 cardiac cells [18], and hypoxia inducing cardiac fibroblast proliferation and phenotypic switch are caveolin-dependent in *in vitro* and *in vivo* models of ischemic injury [19].

We previously reported that pretreatment with total saponin of red ginseng, i.e., purified extract of steamed *Panax ginseng* (EPG), attenuated $[Ca^{2+}]_i$ overload in MI injury [20], however, the underlying mechanisms remain largely unknown. Ginsenosides, except ginsenoside Ro, are the steroid-like saponins [21]. Thus, we hypothesized that EPG could affect caveolin-1 phosphorylation through ginsenosides and further regulate $SOCE/[Ca^{2+}]_i$. Hence, in the present study, the impact of inhibiting caveolin-1 phosphorylation on EPG against cardiac apoptosis and fibrosis following MI and the underlying mechanism were explored both *in vitro* and *in vivo*.

2. Materials and methods

2.1. Reagents and materials

The six-year-old red ginseng was purchased from Jilin Kangmei Xinkaihe Pharmaceutical Co., Ltd (Jilin, China) and authenticated by associate professor Chenxue Pan of Zhengzhou University. Ginsenoside Rg1, Re, Rf, Rb1, Rc, Rg2, Rh1, Rb2, Rb3 and Rd (purity > 98%) were obtained from Chengdu Must-Biotechnology Co., Ltd. (Chengdu, China). Antibodies of phospho-caveolin-1 (Tyr14) and caveolin-1 were obtained from Affinity Biosciences and Bioss Inc. (Beijing, China), respectively. Antibodies of GAPDH, and ORAI1, TRPC1 and STIM1 were purchased from Servicebio, and Boster Biological Technology, Wuhan, China, respectively. Terminal deoxynucleotidyl transferase-mediated dUTP nick end labeling (TUNEL) detection Kit and Masson Stain Kit were provided by Servicebio, Wuhan, China. Other chemicals, such as 3-(4-chlorophenyl)-1-(1,1-dimethethyl)-1H-pyrazolo[3,4-d] pyrimidin-4-amine (PP2), and 2,3,5-triphenyltetrazolium (TTC) et al, were obtained from reputable sources.

2.2. Preparation and analysis of EPG

EPG was obtained according to our previous method [20]. Ginsenosides were analyzed by HPLC using Inertex C_{18} column (5μm, 250mm × 4.6mm). The chromatographic conditions are: flow rate, 1.0 ml/min; detection wavelength, 203 nm; the column temperature, 30°C; gradient elution of acetonitrile (A) and water (B), 0-

20min, 19% A; 20-40min, 19-29% A; 40-55min, 29%A; 55-75min, 29-40% A; 75- 78min, 40-50%A. The contents of ginsenoside Rg1, Re, Rf, Rb1, Rc, Rg2+Rh1, Rb2, Rb3 and Rd were 9.62%, 3.93%, 3.14%, 13.08%, 12.71%, 3.38%, 7.37%, 0.98% and 3.75%, respectively, accounting for 57.96% in EPG (Supplementary Fig.1).

2.3. Primary culture of neonatal rat cardiomyocytes and cell viability assay

The neonatal rat cardiomyocytes were obtained and cultured following the reported method [20]. They were starved by serum-free DMEM 24 h before experiments. Cell viability were assessed by cell counting Kit-8 (CCK-8) assay. Optical density (OD) value was detected at 450 nm with a microplate reader (Thermo, USA). Cells viability (%) = (OD sample - OD blank) / (OD control - OD blank) × 100%.

2.4. Inducement of hypoxia injury

The hypoxia model of cardiomyocyte was induced by the AnaeroPack system as previously published [22]. Briefly, cells were placed inside a sealed airtight container with an AnaeroPack (Mitsubishi Gas Chemical, Tokyo, Japan) to generate hypoxic atmosphere by absorbing oxygen and producing carbon dioxide.

2.5. Drug treatment

Caveolin-1, as a Src tyrosine kinase substrate, can be activated by Src and phosphorylated (Tyr14). PP2, a specific Src inhibitor, blocks caveolin-1 phosphorylation [23]. After cells were pretreated by PP2 (10 μM) for 10 min to inhibit caveolin-1 phosphorylation, they were maintained in the presence or absence of 200 μg/mL EPG for 10 h and followed by hypoxia for 6 h. Then cell viability was determined.

2.6. Measurement of myocardial injury biomarkers

The culture medium and the serum were collected and analyzed by lactate dehydrogenase (LDH) kit (Jiancheng Bio, Nanjing, China), B-type natriuretic peptide (BNP) ELISA kit (Zci Bio, Shanghai, China) and cardiac Troponin I (cTnI) ELISA kit (Novatein Bio, USA) according to the instructions.

2.7. Measurement of $[Ca^{2+}]_i$ concentration

Fluo-3 AM (Solarbio, Beijing, China) was used to detect $[Ca^{2+}]_i$. The cells were loaded with Fluo-3 AM (5 μM) for 30 min at room temperature in phosphate-buffered saline (PBS), then washed with PBS. The change in Ca^{2+} fluorescence intensity was assessed with excitation 488 nm and emission 530 nm.

2.8. Animals and experimental protocols

Male SD rats weighing 220-250g were purchased from Laboratory Animal Center of Henan (Henan, China) and housed at 25 ± 1°C and 50% humidity, with light-dark cycle of 12 h and free access to food and water. All protocols involving animals were approved by the Laboratory Animal Ethics Committee of Zhengzhou University and carried out according to the Guidelines of the Care and Use of Laboratory Animals.

Rats were divided randomly into five groups with 10 animals per group: sham, MI, 200 mg/kg EPG (body wt.), 10μg/kg PP2 + 200 mg/kg EPG, and 10.8 mg/kg diltiazem as a positive control of a Ca^{2+} channel blocker. We previously reported that compared with the model group, pretreatment with EPG showed a dose-dependent reduction in infarct size at dose of 50, 100, 200, 400 mg/kg, and

200 and 400 mg/kg EPG significantly decreased the infarct size ($P < 0.05$), therefore 200 mg/kg EPG, the minimal effective dosage, was used in the present study [20]. EPG and diltiazem were administered by gavage twice daily for seven consecutive days prior to heart ischemia operation. Rats in EPG + PP2 group were injected with PP2 through caudal vein 20 minutes before each time administration of EPG. The sham and MI rats received an equal volume of vehicle that dissolved the drug.

2.9. Acute myocardial ischemia (AMI) rat model

AMI injury of rats was conducted as reported previously [20] through ligating the left anterior descending coronary artery (LAD). The sham group underwent all procedures without ligation of LAD. After 24h of AMI, the blood was sampled from the abdominal aorta and centrifuged at 3000 rpm for 15 min for obtaining serum, the heart was collected and rinsed with ice-cold PBS (pH 7.4).

2.10. Determination of infarct size

Myocardial infarct sizes were determined using TTC staining, as described previously [20]. After the pictures were taken, the formula: Infarct size (%) = (infarct area/whole heart area) × 100%, was used to normalize.

2.11. Hematoxylin and eosin (HE) staining and masson staining

The hearts fixed in 4% paraformaldehyde for 48 h were subjected to gradient dehydration, transparency and paraffin embedding. Crosswise 3 μm-thick heart sections were cut and stained by HE and Masson staining according to their respective standard protocols. Fibrosis area (%) = (area of collagen fibers/ area of muscle fibers and collagen fibers) × 100%.

2.12. TUNEL staining

TUNEL staining was carried out according to the manufacturer's protocols. The nuclei positive for TUNEL staining were counted in five randomly chosen fields in a blind manner and expressed as the percentage of the total number of cardiomyocytes.

2.13. Transmission electron microscopy (TEM)

Cardiac tissue at the apex of the left anterior wall were taken and cut into small pieces ($1 \ mm^3$) and fixed in electron microscopy fixation buffer for 24 h (4 °C). After the samples were washed with PBS, fixed in 1% osmium tetroxide in PBS for 1 h, dehydrated, and then permeated and embedded. Next, the ultrathin sections were cut and stained with 2% uranyl acetate and lead citrate for 15min, respectively, and dried and photographed by a HT7800 TEM (Hitachi, Ltd., Tokyo, Japan) operating at 120 kV.

2.14. Immunofluorescence

After antigen retrieval was performed on the tissue sections, they were blocked for 30 min with 3% bovine serum albumin and incubated with primary antibody against p-caveolin-1 (#AF3386), or STIM1 (#PB9406) and fluorescent secondary antibody. Next, sections were stained for 10 min with DAPI staining, washed with PBS, and then photographed with a fluorescence microscope.

2.15. Western blotting analysis

The total proteins were extracted from homogenized heart tissue using RIPA lysis buffer with 1% phosphatase and 1% protease inhibitors (Beyotime, Shanghai, China), and quantified by BCA kit (Solaibao, Beijing, China). Equal amounts of proteins were separated using 12% SDS-PAGE and transferred onto membranes. After the membranes were blocked and incubated with primary antibodies against caveolin-1 (1:1000; #bs-1453R), p-caveolin-1 (1:1000), ORAI1 (1:1000; #A00909), TRPC1 (1:1000; #M01492), STIM1 (1:1000), and GAPDH (1:2000; #GB11002), they were wash and incubated with secondary antibodies (1:10000, #BE0101, Bioeasy, Shanghai, China). Finally, the bands were visualized using ECL (Millipore, USA), and normalized to GAPDH.

2.16. Quantitative real-time polymerase chain reactions (qRT-PCR)

Total RNA was extracted from homogenized rat cardiac tissues using the animal total RNA Isolation Kit (Cwbio, Beijing, China) and quantified with the Nanodrop 2000 spectrophotometer (Thermo Scientific, Shanghai, China). 1 μg of total RNA was reverse transcribed into cDNAs with the Servicebio®RT First Strand cDNA Synthesis Kit (Servicebio, Wuhan, China), qRT-PCR were run on the CFX Connect™ Real-Time System (BIO-RAD, USA). Primer for RT-PCR are designed and synthesized by Servicebio, and the sequences are listed in Table 1. Data of mRNA were normalized to GAPDH expression.

2.17. Statistical analysis

All data are presented as the means ± standard deviation (SD). Student's t-test or one-way analysis of variance (ANOVA) were used. $P < 0.05$ was considered statistically significant.

3. Results

### 3.1. EPG inhibited hypoxia injury in cardiomyocytes

The AnaeroPack System treatment caused a time-dependent decrease in cardiomyocyte viability (Fig. 1A); LDH could be detected only in the group treated for 6h (data not shown); therefore, 6 h was selected as the optimal hypoxia time for further experiments of cells. Prior to the hypoxia treatment, cells were pretreated by EPG at 100 - 400 μg/mL of EPG for 10 h, a concentration-dependent increase of survival was observed, and starting from 200 μg/mL, the increase has a significant difference (Fig. 1B). Therefore, 200 μg/mL was used for subsequent researches.

3.2. Protective effect of EPG on hypoxia injury involved in p-caveolin-1 in cardiomyocytes

As shown in Fig. 1C–F, PP2 (10 μM), an inhibitor of caveolin-1 phosphorylation, hardly affected the hypoxic cells, however

Table 1
Primer Sequence of qRT-PCR

Genes	Forward Primer sequence	Reverse Primer sequence
Caveolin-1	TGTCTATTCCATCTACGTCCAC	TCATATCTCTTTCTGCGTGCTG
ORAI1	AAAGCCTCCAGCCGAACCT	AAAAGCAGCGTCCCGATGAC
TRPC1	AAAAAGGACAGCCTCAGACATTC	GCACTAAGTTCAAACGCTCTCAG
STIM1	GGATCTCAGAGGGATTTGACCC	CATTGGAAGACGTGGCATTGA
GAPDH	CTGGAGAAACCTGCCAAGTATG	GGTGGAAGAATGGGAGTTGCT
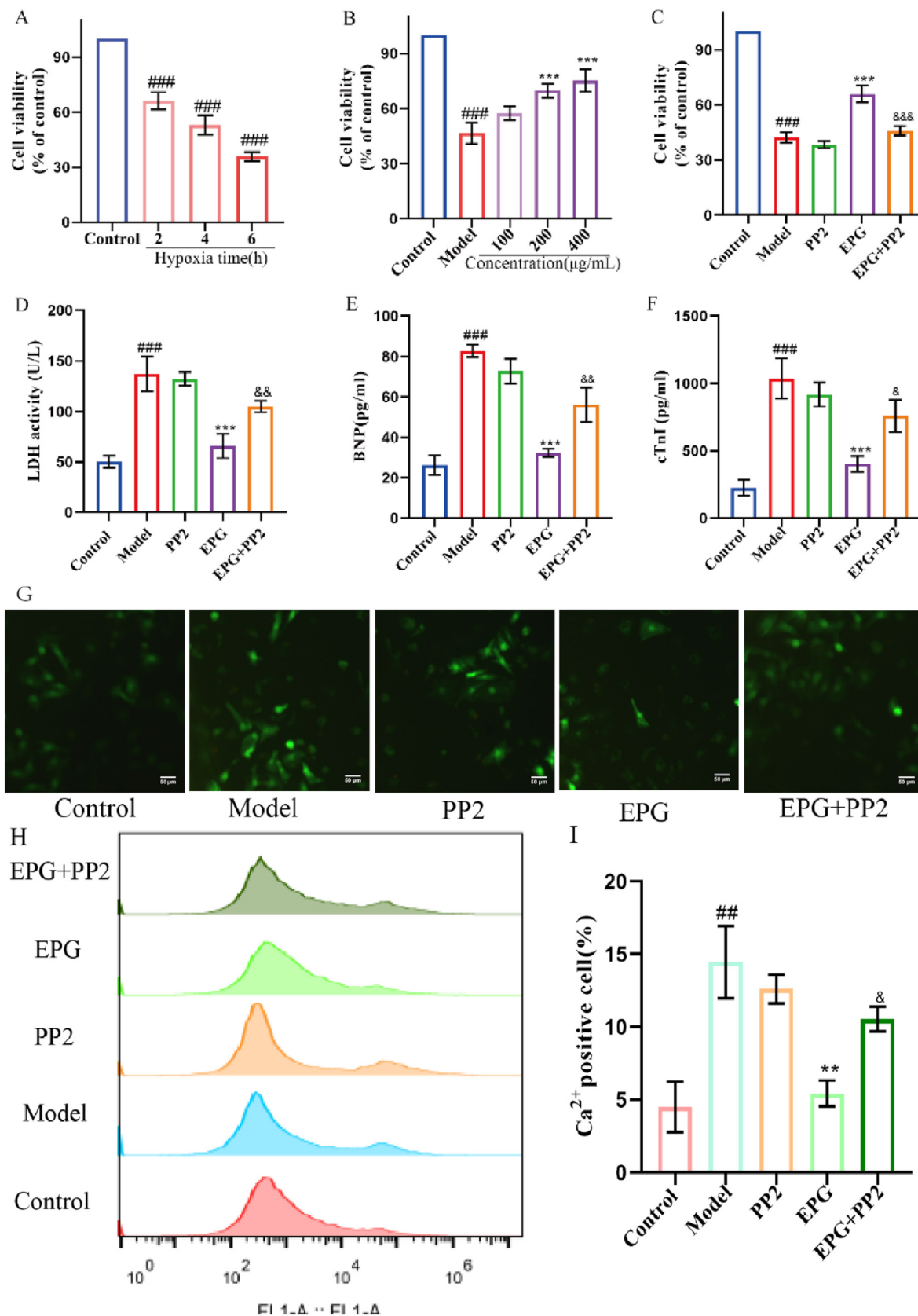
Fig. 1. EPG increased viability, and reduced injury biomarkers and [Ca2+]i in hypoxia cardiomyocytes via p-caveolin-1 (three independent experiments done in quintuplicate). Effect of hypoxia time (A) and EPG doses under hypoxia for 6 h (B) on cells. Effect of PP2 on cells (C) and LDH, BNP and cTnI (D-F) under 200 μg/mL EPG. Fluo-3 fluorescence measured by microscope (G) and flow cytometry (H, I). ###P < 0.001, ##P < 0.01 vs. normal control; ***P < 0.001, **P < 0.01vs. model, & P < 0.05, && P < 0.01, &&& P < 0.001 vs. EPG.

pretreatment with EPG significantly enhanced cell viability, reduced release of LDH, BNP and cTnI; meanwhile, these improvements by EPG were significantly deteriorated after cells were pretreated by PP2; suggesting p-caveolin-1 may be involved in the protection of EPG.

3.3. EPG decreased $[Ca^{2+}]_i$ via p-caveolin-1 in cardiomyocytes

Because phosphorylation of caveolin-1 can inhibit Ca^{2+} influx [17], we wondered whether the protective effect of EPG via p-caveolin-1 was related to $[Ca^{2+}]_i$. The fluorescence of $[Ca^{2+}]_i$ in hypoxia cardiomyocytes became stronger compared with the normal control, and was hardly influenced by PP2 (Fig. 1G). EPG preconditioning decreased the fluorescence of hypoxia cells, which was enhanced again in PP2 + EPG group. The Ca^{2+} positive cardiomyocytes in flow cytometry assay, represented by the peak on the right in Fig. 1H, have a significantly higher percent in hypoxia model than normal control (Fig. 1 I). Compared with model group, the percent was hardly affected by PP2, but significantly decreased by EPG to 5.43%. In PP2+EPG group, the percent increased to 10.56% with significant difference with EPG. A lower percent indicates a less cardiomyocytes injury. The results suggested that EPG attenuated Ca^{2+} influx via p-caveolin-1 in hypoxic cardiomyocytes.

3.4. Inhibition of caveolin-1 phosphorylation weakened EPG improvement against myocardial infarct and myocardial injury biomarkers in rats

Myocardial infarct size of model was significantly bigger than that of the sham (Fig. 2A and B). Compared with the model, both EPG and positive drug diltiazem could significantly reduce the myocardial infarct size ($P < 0.001$). However, the decrease was

significantly increased by the use of PP2 to suppress the caveolin-1 phosphorylation in PP2 + EPG group, suggesting the protection of EPG against myocardial infarct was mediated, at least partly, by caveolin-1 phosphorylation.

LDH, BNP, and cTnI were significantly increased in the model rats. EPG pretreatment resulted in significant reduction, their levels were significantly higher in PP2+EPG compared with EPG (Fig. 2C–E). The results further indicated that p-caveolin-1 was associated with EPG protection.

3.5. EPG inhibited cardiac apoptosis via caveolin-1 phosphorylation in rats

Excessive apoptosis contributes to cell death invariably following ischemia stress [24]. Fig. 3A,C showed that apoptotic TUNEL positive cells were greatly increased in the cardiac tissues of model rats compared with that in the sham group; pretreatment with EPG or diltiazem significantly decreased the percent of TUNEL positive cells when compared with the model group; however, the cardiac apoptosis was significantly increased in PP2+EPG group compared with the EPG group ($P < 0.001$); indicating that EPG exerts anti-apoptotic effect in rat heart via caveolin-1 phosphorylation.

3.6. EPG decreased STIM1 via caveolin-1 phosphorylation against ischemic injury in rats

Given inhibition of p-caveolin-1 significantly lowered EPG-mediated cardiomyocytes protection and $[Ca^{2+}]_i$ was involved in, the STIM1 as Ca^{2+} sensor would also be expected to be related. Therefore, the expression of p-caveolin-1 and STIM1 in heart tissue were examined by immunohistochemical staining. After MI,
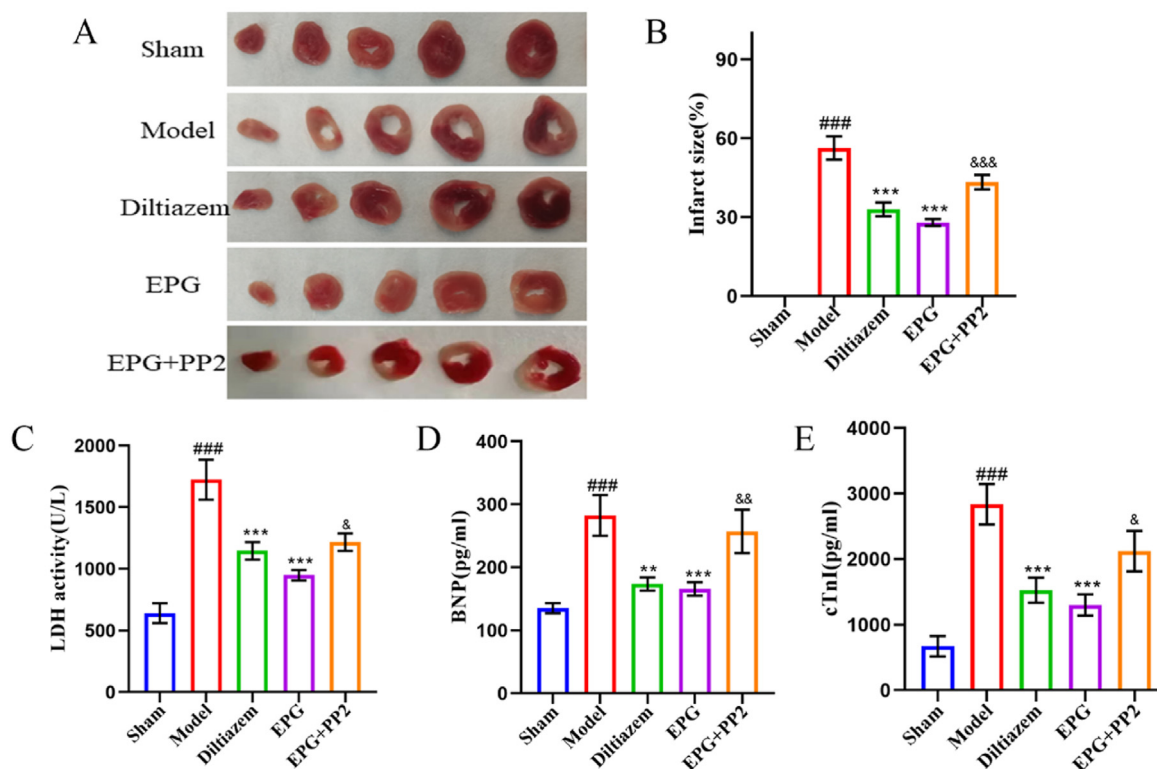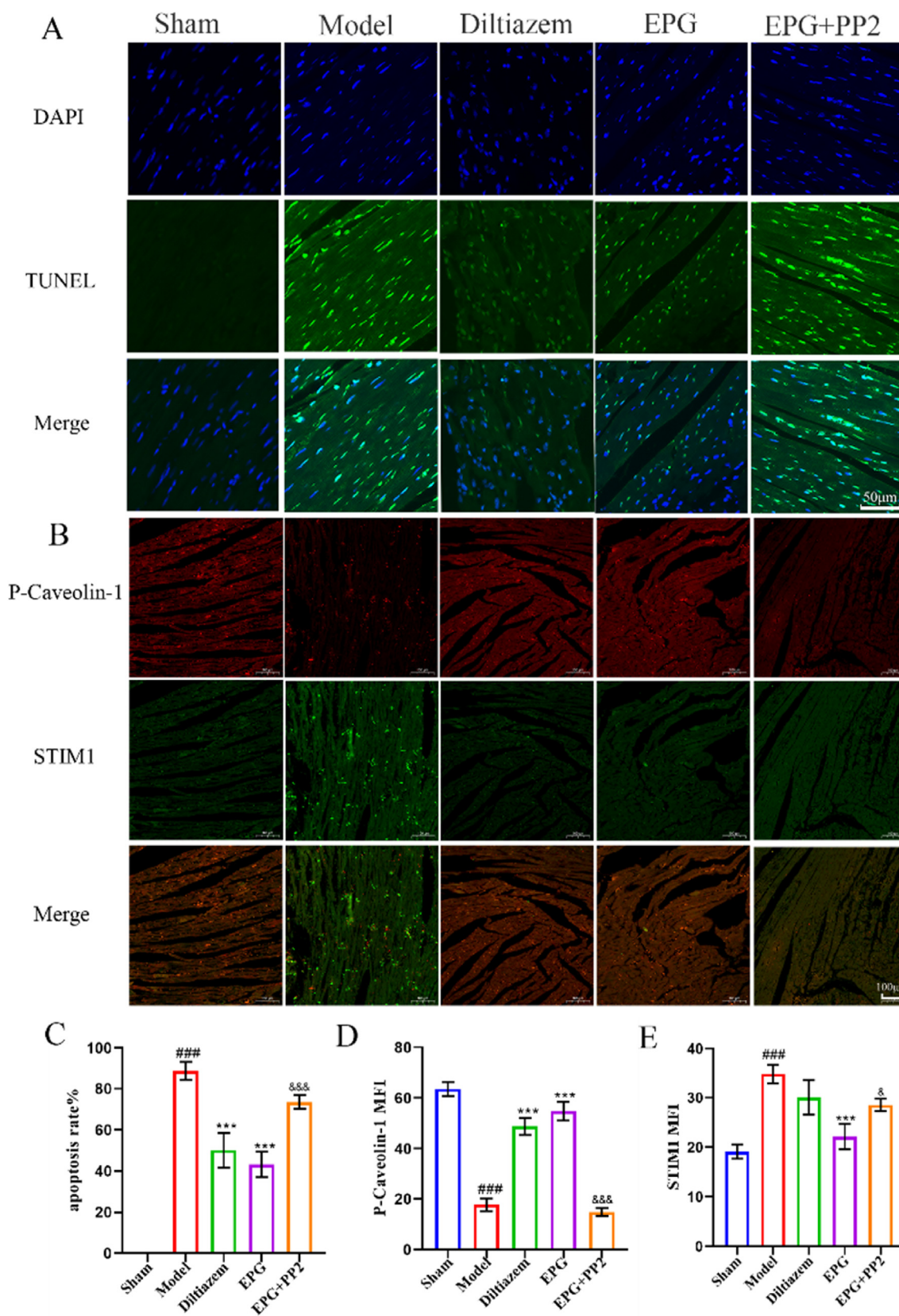

Fig. 2. EPG improved myocardial infarct and injury biomarkers in rats with MI via p-caveolin-1 (n = 6-10/group). (A) TTC staining. (B) Infarction size (%). (C-E) Release of LDH, BNP and cTnI (C-E). ###P < 0.001 vs. sham; **P < 0.01, ***P < 0.001, vs. model; &P < 0.05, &&P < 0.01, &&&P < 0.001 vs. EPG.

Fig. 3. EPG inhibited apoptosis and decreased STIM via p-caveolin-1 against MI injury in myocardium of rats (n = 4-6/group). (A) TUNEL staining, apoptotic nuclei (green) and DAPI-positive normal nuclei (blue). (B) Immuno-histochemical staining of p-caveolin-1 and STIM1. (C) Apoptotic rate (%). (D, E) Quantitative mean fluorescence intensity (MFI). ###$P < 0.001$ vs. sham, ***$P < 0.001$ vs. model, & $P < 0.05$, &&&$P < 0.001$ vs. EPG.

fluorescence intensity of p-caveolin-1 and STIM1 were dramatically weaker and stronger ($P < 0.001$), respectively (Fig. 3B and D, E). Compared with the model, the fluorescence of p-caveolin-1 and STIM1 were significantly increased and decreased by EPG, and showed significantly enhanced and a decrease tendency in diltiazem, respectively. Meanwhile, PP2+EPG group displayed lower p-caveolin-1 and higher STIM1 fluorescence intensity than the respective EPG group with significant differences between them, suggesting that EPG exerts cardioprotective effects by decreasing STIM1 expression *via,* at least partly, p-caveolin-1 expression.
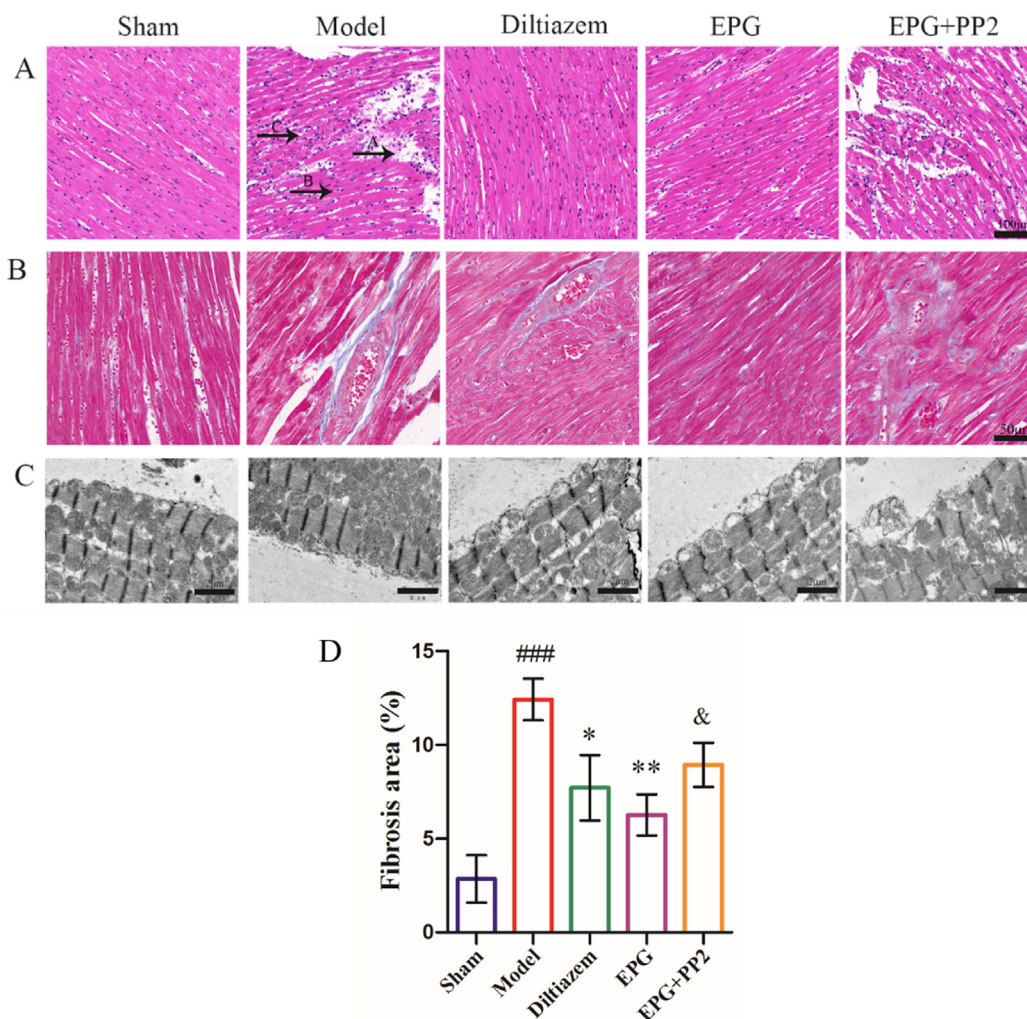
3.7. EPG attenuated cardiac pathological damages in rats

HE staining (Fig. 4A) showed that cardiomyocytes of sham group were arranged regularly, transverse striation was clear and ordered, and intercellular space was uniform, however, cardiomyocytes of model group swelled and showed extensive necrotic myocardial tissue with inflammatory cells infiltration, intercellular space expanded and the cardiac structure was disordered. EPG or diltiazem pretreatment improved these damages. Whereas these ameliorated effect by EPG was attenuated in the PP2+ EPG group,

cardiomyocytes of rats showed edema, deep nuclear staining of nuclear condensation, and transverse striation was disordered.

The Masson staining (Fig. 4B) showed myocardial tissue of sham group was normal in structure, uniformly stained, and had occasional fibrosis, however, the extensive collagen deposition was observed in model group, and significant difference was found between model group (12.42%) and sham group (2.85%) in percent of fibrosis (Fig. 4D). Pretreatment with EPG and diltiazem significantly relieved MI-induced fibrosis, but fibrosis was increased in PP2+EPG group compared with EPG group and there was significant difference between them.

TEM showed mitochondria were arranged regularly under the myofilament and their structure were normal and clear in the sham group (Fig. 4C). After AMI, mitochondria are unevenly distributed and clustered in some regions, and showed pathological changes such as irregular shape and swelling, mitochondrial cristae injury and breakage. EPG or diltiazem improved the mitochondria disorders of myocardium. Whereas PP2+EPG group markedly reversed the improvement by EPG. In short, the above results of pathology suggested that the amelioration effects of EPG on MI was related to the caveolin-1 phosphorylation.

Fig. 4. EPG improved cardiac pathological damages in rats with MI (n = 4-6/group). (A) HE staining, Arrows A, B and C indicate myocardial fiber rupture, cells swelling, and inflammatory infiltration, respectively. (B) Masson staining, myocardial fibers (red) and collagen fibers (blue). (C) TEM. (D) Myocardial fibrosis area (%) of Masson staining. ###P < 0.001 vs. sham, **P < 0.01, *P < 0.05 vs. model. & P < 0.05 vs. EPG.

### 3.8. P-caveolin-1-dependent regulating SOCE mediated cardioprotection of EPG against MI in rats

Since EPG decreased the levels of STIM1 *via* p-caveolin-1 against MI, and STIM1 is an important component of SOCE, SOCE should be involved in the protective effect of EPG. As expected, the protein levels of ORAI1, TRPC1 and STIM1 were significantly increased by MI (Fig. 5A, D-F), and EPG manifestly suppressed all of them compared with the model. Diltiazem was also effective in decreasing these protein levels. However, these protein levels were increased to 1.26, 1.17 and 1.01 folds in PP2+EPG rats from 0.99, 0.89 and 0.71 folds in EPG rats, respectively, with significantly difference for all of them between the two groups. And, after MI, the protein levels of caveolin-1 and p-caveolin-1 were significantly decreased (Fig. 5B and C). In accordance with the results of immunohistochemical staining, compared with the model group, p-caveolin-1 protein was significantly increased by EPG and dilti-azem, and was significantly reduced in PP2+EPG group compared with EPG group. Besides, caveolin-1 protein, which had a growing trend in EPG, was significantly decreased in the PP2+EPG group compared with EPG group. These data indicate that p-caveolin-1-dependent regulating SOCE plays a vital role in the cardioprotection of EPG against MI.

As shown in Fig. 5 G-J, STIM1, ORAI1 and TRPC1 mRNA were significantly increased and caveolin-1 mRNA was significantly decreased after MI. EPG significantly decreased ORAI1 mRNA

expression compared with model. And the ORAI1 mRNA in the PP2+EPG group was significantly enhanced compared to the EPG group. The results of proteins and mRNA indicate EPG exerts car-dioprotective effect by regulating ORAI1, TRPC1 and STIM1 proteins *via* p-caveolin-1protein, as well as the ORAI1 mRNA.

4. Discussion

P. ginseng is usually supplemented for disease prevention due to its remarkable tonifying effects. In healthy adults, it improved self-perception of fatigue and energy [25], reduced drop jump-related muscle injury markers [26], augmented the improvement of aero-bic capacity by exercise training [27], and attenuated lymphocyte DNA damage and low-density lipoprotein oxidation [28]. Mean-while, some clinical trials from healthy individuals show no effect: there are no effect on anaerobic capacity and fatigue recovery [29], glucose regulation [30], and neither hepatoprotective nor hepato-toxic effects [31]. However under pathological condition, ginseng exhibits various therapeutic properties, such as against cardiovas-cular diseases [32] and hepatoprotection [31] et al. Further, sub-group analysis showed a greater effect in subjects with prehypertension or hypertension than healthy individuals [33]. These results suggest that human body in health and disease re-sponds differently to ginseng supplement. Therefore, the selection of appropriate model is important. In the present study *in vitro*, AnaeroPack System, a physical method of inducing hypoxia injury,
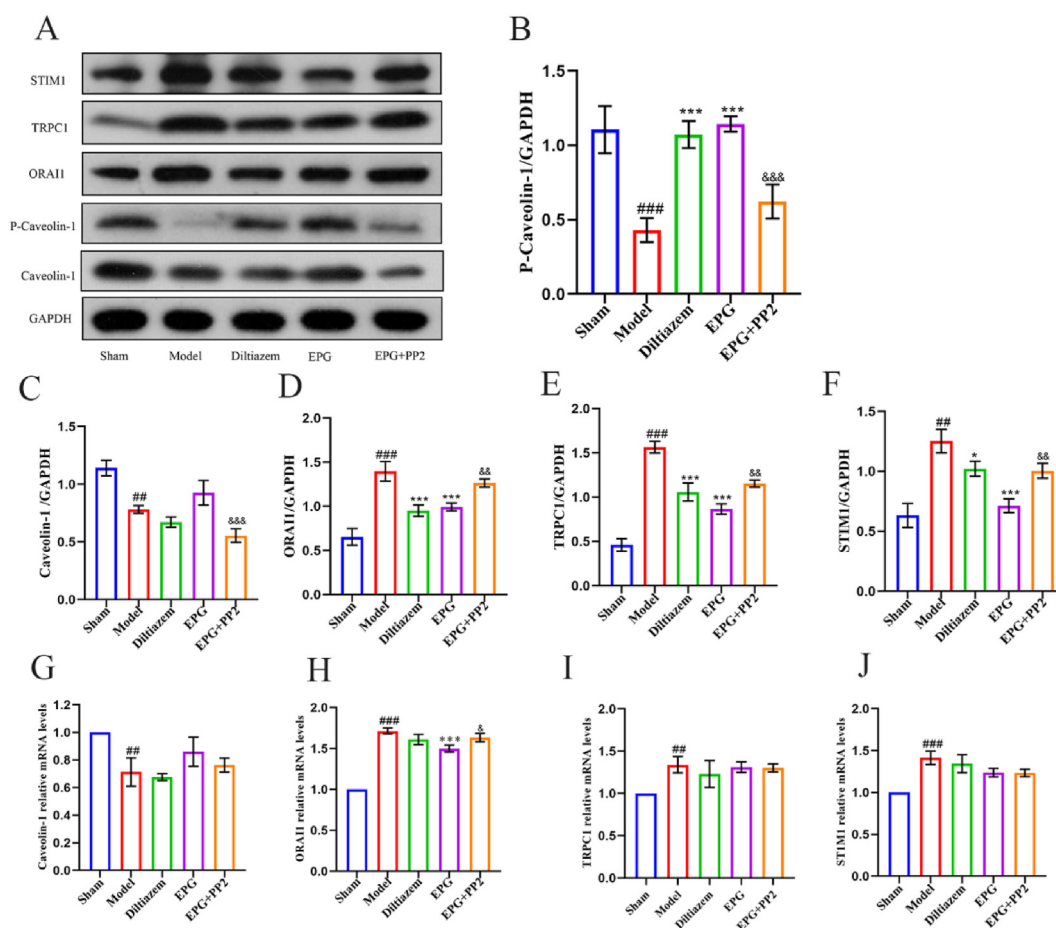
Fig. 5. P-Caveolin-1/SOCE pathway mediated EPG-induced protection against MI injury in rats (n = 4-6/group). (A) Western blot bands. Quantitative analysis of protein expression (B–F) and mRNA expression (G-J). ##P < 0.01, ###P < 0.001 vs. sham; *P < 0.05, ***P < 0.001 vs. model; &P < 0.05, && P < 0.01, &&& P < 0.001 vs. EPG.

was used, which is different from the chemical method we used before [20], to make the research be closer to the actual situation of MI.

P-Caveolin-1 alters the properties of caveolin-1, which is vital to mobilize endogenous protection of IPC and pharmacological pre-conditioning against MI injury [15,16,34]. After IPC and isoflurane preconditioning, mice hearts showed rapid phosphorylation of caveolin-1; but PP2 reduced caveolin-1 phosphorylation and abolished isoflurane-induced cardiac protection [35]. Moreover, caveolin-1 knockout reduced survival in mice subjected to LAD ligation [36]. In keeping with these reports, we found that EPG-induced protection along with increased p-caveolin-1 (Fig. 3B, D and Fig. 5A and B) was significantly reduced after PP2 used (Figs. 1C and 2A, B). Caveolin-1 is an integral component of caveolae, a special form of lipid raft enriched in cholesterol, it is plausible that ginsenosides, similar to cholesterol in structure [21], might interact with cholesterol and affect caveolin-1 properties. Reports have showed that Rp1, a ginsenoside derivative, and ginsenoside Rh2 changed lipid raft distribution [37].

One of the most specific markers for cardiac injury is cTnI [38]. And BNP, a cardiac hormone produced mainly by ventricular myocytes, is significantly positive correlation with clinical out-comes of MI [39]. In addition, cell necrosis can be determined by LDH release assay. These biomarkers were significantly lessened by EPG pretreatment after hypoxic/ ischemic injury (Fig. 1D—F and 2C-E). But, the decrease was significantly attenuated by PP2 adminis-tration, further confirming that EPG has the similar protective effect on MI injury as pharmacological preconditioning *via* p-caveolin-1.

Myocardial damage is closely related to Ca^{2+} overload [1], and caveolin-1 belongs to one of key regulators of the $[Ca^{2+}]_i$ homeo-stasis [17]. Consistent with these reports, EPG significantly rescued hypoxia injury by inhibiting Ca^{2+} influx *via* caveolin-1 phosphor-ylation, which is confirmed by PP2 use (Fig. 1C—I and Fig. 2). Given the effect of EPG on $[Ca^{2+}]_i$, diltiazem, a Ca^{2+} channel blocker, was chosen as a positive drug in the experiment of rats.

During cardiac excitation contraction coupling in normal car-diomyocytes, the voltage-gated L-type Ca^{2+} channels (LTCC) are triggered to open, thereby allowing a small amount of Ca^{2+} to enter the cell, which in turn triggers the release of a much greater amount of Ca^{2+} from SR and gives rise to the systolic Ca^{2+} transient and contraction. The persistent increases in Ca^{2+} influx through the LTCC enhances contractility but leads to apoptosis by inducing SR Ca^{2+} overload [40]. Ginsenosides mainly may play an inhibitory role in LTCC in normal cardiomyocytes and thereby prohibiting influx of Ca^{2+}: panaxadiol saponins, panaxatriol saponins, and ginsenoside Rb1, Rb2, Rb3 and Rc had blockade effect on LTCC [41], ginsenoside Re, Rb1 and Rd suppressed LTCC current ($I_{Ca,L}$) [42—44]. Moreover, in *Xenopus* oocytes expressing cardiac L(α_{1C})-type Ca^{2+} channels, ginseng total saponins and ginsenoside Rg3, Rh2 exerted inhibitory effect (Rh2 >Rg3> total saponins) [45]. Importantly, ginsenoside, such as Rb1, can inhibit the opening of LTCC in ischemic cardiomyocytes [44]. Therefore, the anti-apoptosis induced by EPG and diltiazem (Fig. 3A, C) *via* inhibiting Ca^{2+} influx (Fig. 1G—I) may partly attribute to inhibit LTCC. Besides, accumulating evidences have indicated that approaches aimed at SOCE (comprising STIM1, ORAI1 and TRPC), a major mechanism of Ca^{2+} entry from extracellular in cardiovascular disease, may be therapeutic [5].

Inhibition of STIM1-induced $[Ca^{2+}]_i$ accumulation exerted anti-apoptotic activity in cardiomyocyte of hypoxia/reoxygenation damage [46]. Moreover, knockdown of TRPC1 significantly allevi-ated myocardial apoptotic injury [47]. Therefore, the decrease of $[Ca^{2+}]_i$ induced by EPG *via* p-caveolin-1 (Fig. 1G—I) inhibiting STIM1 and TRPC1 (Fig. 3B,E and Fig. 5A, E, F) may be one of the potential mechanisms underlying the anti-apoptosis effect.

Excessive apoptosis can promote MI [24]. The anti-apoptosis effect of EPG partly accounted for its rescue activity on MI rats (Fig. 3A and B). Similar to our present study, ginsenosides and ginsenoside Rg1 [48], which is up to 9.62% in EPG, had been proven to inhibit myocardial cell apoptosis against I/R injury.

STIM1 activates TRPC1 via its C-terminal polybasic domain, which is distinct from its ORAI1-activating domain; and knock-down of STIM1 dramatically reduces TRPC1-mediated SOCE and Ca^{2+} current [7]. Moreover, the transgenic mice with STIM1 over-expression in the heart showed enhanced Ca^{2+} entry following store depletion, and developed sudden cardiac death or heart failure [8]. Therefore, STIM1 activation is a necessary step for the opening of SOCE. Our results demonstrated that decrease of STIM1 was involved in myocardial protection of EPG following MI (Fig. 3B, E and Fig. 5A, F). In addition, EPG-induced STIM1 decrease can be reversed by the inhibition of p-caveolin-1 (Fig. 3 B, E and Fig. 5A, B, F), suggesting that caveolin-1 was the upstream of STIM1 in the protection of EPG against MI.

Caveolin-1 contributes to assembly of SOCE channels by regu-lating plasma membrane localization of TRPC1 *via* an interaction between N terminus of TRPC1 and caveolin-1; importantly, disruption of TRPC1 localization suppressed SOCE [49]. Moreover, caveolin-1 can interact with the STIM1-ORAI1 complex to increase activity of SOCE [17]. Furthermore, STIM1-ORAI1-TRPC1 complex might be involved in SOCE activation due to knockdown of any of the three proteins reducing SOCE [7]. The amelioration of EPG and diltiazem on $[Ca^{2+}]_i$ is mainly due to increasing p-caveolin-1 pro-tein and decreasing STIM1, ORAI1 and TRPC1 proteins (Fig. 5A—F); and after PP2 used, these improvements by EPG were significantly deteriorated and the decreased expression level of ORAI1 mRNA by EPG was again enhanced (Fig. 5H). Therefore, EPG-regulated p-caveolin-1 may alter the interaction between caveolin-1 and SOCE, and thus inhibits the Ca^{2+} influx, which are in consistent with the above-mentioned studies and the report of p-caveolin-1 inhibiting Ca^{2+} influx [17].

Caveolin-1 is important for maintaining normal mitochondrial structure of cardiomyocytes after ischemic injury [50]. Moreover, gobal caveolin-1 knock-out mice altered cardiac mitochondrial function and increases susceptibility to stress [51]. Furthermore, SR and mitochondria are dynamic organelles constantly communi-cating with each other, thus mitochondria play a major role in Ca^{2+} buffering to modulate apoptosis in a concerted manner with SR [52]. EPG improving the abnormalities of mitochondrial ultra-structure *via* p-caveolin-1 (Fig. 4C) may ascribe to the decrease of $[Ca^{2+}]_i$ *via* p-caveolin-1 inhibiting STIM1 of SR (Fig. 3B, E and Fig. 5A, F).

Caveolin-1$^{-/-}$ gene knockout mice exacerbated cardiac fibrosis after MI, and cardiac remodeling can be improved by restoring caveolin-1 function in wild-type MI mice [53]. And, maintenance of $[Ca^{2+}]_i$ homeostasis through cardiac-specific overexpression mito-chondrial Ca^{2+} uniporter to uptake Ca^{2+} suppressed heart fibrosis [4]. The decrease of myocardial fibrosis by EPG (Fig. 4B, D) *via* p-caveolin-1 reducing $[Ca^{2+}]_i$ (Fig. 1G—I) is in agreement with these reports. Ginsenoside Rg2, Rg3 and Re improved myocardial fibrosis in isoproterenol-induced MI rats by inhibiting TGF-β1/Smad signaling pathway [54—56], suggesting other than caveolin-1 might also play a role in the effect of EPG on anti-fibrosis.

The abnormalities of platelet activity, whole blood viscosity (WBV) and blood pressure (BP), also contribute to MI. Red ginseng extract and its components, such as ginsenoside Rk1, Rg1, Rg3, F4, Rp1, Rp3, Rp4 and gintonin, have been reported to inhibit platelet aggregation [57]. And, water decoction of ginseng significantly reduced the WBP viscosity *in vivo* and *in vitro* [58]. In addition, although hypertension is one of major risk factors of MI, excessive diastolic pressure drops may jeopardize coronary perfusion.

Notably, red ginseng had bidirectional regulation effects on BP, i.e., not only reducing BP in patients with pre-hypertension and hypertension in acute and long-term [33], but also ameliorating low BP in patients with hypotension for restoring to normal level [59]. Moreover, improvement of EPG on the coronary blood flow was confirmed by us in AMI dogs [60]. These benefits may also help cardioprotection of EPG.

Overall, inhibition of the caveolin-1 phosphorylation significantly decreased the cardioprotective effects of EPG. Mechanistically, the suppression of SOCE/$[Ca^{2+}]_i$ signaling pathway *via* p-caveolin-1 was, at least partially, involved in. These findings, for the first time, implicate that caveolin-1 phosphorylation mediates the protective effects of EPG against MI injury.

Declarations

Journal of Ginseng Reaearch requires that all authors sign a declaration of conflicting interests. If you have nothing to declare in any of these categories then this should be stated.

Please state any competing interests

The authors declare that there are no conflicts of interest.

Funding source

Please state any sources of funding for your research

Declaration of competing interest

A conflicting interest exists when professional judgement concerning a primary interest (such as patient's welfare or the validity of research) may be influenced by a secondary interest (such as financial gain or personal rivalry). It may arise for the authors when they have financial interest that may influence their interpretation of their results or those of others. Examples of potential conflicts of interest include employment, consultancies, stock ownership, honoraria, paid expert testimony, patent applications/registrations, and grants or other funding.

Acknowledgments

Appendix A. Supplementary data

Supplementary data to this article can be found online at https://doi.org/10.1016/j.jgr.2023.07.003.

References

[1] Schirone L, Forte M, D'Ambrosio L, Valenti V, Vecchio D, Schiavon S, Spinosa G, Sarto G, Petrozza V, Frati G, et al. An Overview of the molecular mechanisms associated with myocardial ischemic injury: state of the art and translational perspectives. Cells 2022;11:1165.

[2] Liu ZY, Zhong QW, Tian CN, Ma HM, Yu JJ, Hu S. NMDA receptor-driven calcium influx promotes ischemic human cardiomyocyte apoptosis through a p38 MAPK-mediated mechanism. J Cell Biochem 2019;120:4872—82.

[3] Ma JQ, Chen ZW, Ma YJ, Xia Y, Hu K, Zhou Y, Chen A, Qian JY, Ge JB. MicroRNA-19a attenuates hypoxia-induced cardiomyocyte apoptosis by downregulating NHE-1 expression and decreasing calcium overload. J Cell Biochem 2020;121: 1747—58.

[4] Wang P, Xu S, Xu J, Xin Y, Lu Y, Zhang H, Zhou B, Xu H, Sheu SS, Tian R, et al. Elevated MCU expression by CaMKIIδB limits pathological cardiac remodeling. Circulation 2022;145:1067—83.

[5] Lu T, Zhang Y, Su Y, Zhou D, Xu Q. Role of store-operated Ca^{2+} entry in cardiovascular disease. Cell Commun Signal 2022;20:33.

[6] Bootman MD, Rietdorf K. Tissue specificity: store-operated Ca^{2+} entry in cardiac myocytes. Adv Exp Med Biol 2017;993:363—87.

[7] Ambudkar IS, de Souza LB, Ong HL. TRPC1, Orai1, and STIM1 in SOCE: friends in tight spaces. Cell Calcium 2017;63:33—9.

[8] Correll RN, Goonasekera SA, van Berlo JH, Burr AR, Accornero F, Zhang HY, Makarewich CA, York AJ, Sargent MA, Chen XW, et al. STIM1 elevation in the heart results in aberrant Ca^{2+} handling and cardiomyopathy. J Mol Cell Cardiol 2015;87:38—47.

[9] Luik RM, Wang B, Prakriya M, Wu MM, Lewis RS. Oligomerization of STIM1 couples ER calcium depletion to CRAC channel activation. Nature 2008;454: 538—42.

[10] Jardín I, Albarran L, Salido GM, López JJ, Sage SO, Rosado JA. Fine-tuning of store-operated calcium entry by fast and slow Ca^{2+}-dependent inactivation: involvement of SARAF. Biochim Biophys Acta Mol Cell Res 2018;1865:463—9.

[11] Collins HE, Zhu-Mauldin X, Marchase RB, Chatham JC. STIM1/Orai1-mediated SOCE: current perspectives and potential roles in cardiac function and pathology. Am J Physiol Heart Circ Physiol 2013;305:H446—58.

[12] Eisner DA, Caldwell JL, Kistamás K, Trafford AW. Calcium and excitation-contraction coupling in the heart. Circ Res 2017;121:181—95.

[13] Nan J, Li J, Lin Y, Saif Ur Rahman M, Li Z, Zhu L. The interplay between mitochondria and store-operated Ca^{2+} entry: emerging insights into cardiac diseases. J Cell Mol Med 2021;25:9496—512.

[14] Norman R, Fuller W, Calaghan S. Caveolae and the cardiac myocyte. Curr Opin Physiol 2018;1:59—67.

[15] Yang Y, Ma Z, Hu W, Wang D, Jiang S, Fan C, Di S, Liu D, Sun Y, Yi W. Caveolin-1/-3: therapeutic targets for myocardial ischemia/reperfusion injury. Basic Res Cardiol 2016;111:45.

[16] Sowa G. Caveolae, caveolins, cavins, and endothelial cell function: new insights. Front Physiol 2012;2:120.

[17] Yeh YC, Parekh AB. Distinct structural domains of caveolin-1 independently regulate Ca^{2+} release-activated Ca^{2+} channels and Ca^{2+} microdomain-dependent gene expression. Mol Cell Biol 2015;35:1341—9.

[18] Takaguri A, Kamato M, Satoh Y, Ohtsuki K, Satoh K. Effect of alteration of caveolin-1 expression on doxorubicin-induced apoptosis in H9c2 cardiac cells. Cell Biol Int 2015;39:1053—60.

[19] Gao Y, Chu M, Hong J, Shang J, Xu D. Hypoxia induces cardiac fibroblast proliferation and phenotypic switch: a role for caveolae and caveolin-1/PTEN mediated pathway. J Thorac Dis 2014;6:1458—68.

[20] Li HX, Han SY, Ma X, Zhang K, Wang L, Ma ZZ, Tu PF. The saponin of red ginseng protects the cardiac myocytes against ischemic injury in vitro and in vivo. Phytomedicine 2012;19:477—83.

[21] Attele AS, Wu JA, Yuan CS. Ginseng pharmacology: multiple constituents and multiple actions. Biochem Pharmacol 1999;58:1685—93.

[22] Wen Z, Mai Z, Zhu X, Wu T, Chen Y, Wang J. Mesenchymal stem cell-derived exosomes ameliorate cardiomyocyte apoptosis in hypoxic conditions through microRNA144 by targeting the PTEN/AKT pathway. Stem Cell Res Ther 2020;11:36.

[23] Bakhshi FR, Mao M, Shajahan AN, Piegeler T, Chen Z, Chernaya O, Sharma T, Elliott WM, Szulcek R, Bogaard HJ, et al. Nitrosation-dependent caveolin 1 phosphorylation, ubiquitination, and degradation and its association with idiopathic pulmonary arterial hypertension. Pulm Circ 2013;3:816—30.

[24] Dong Y, Chen HW, Gao JL, Liu YM, Li J, Wang J. Molecular machinery and interplay of apoptosis and autophagy in coronary heart disease. J Mol Cell Cardiol 2019;136:27—41.

[25] Tardy AL, Bois De Fer B, Cañigueral S, Kennedy D, Scholey A, Hitier S, Aran A, Pouteau E. Reduced self-perception of fatigue after intake of Panax ginseng root extract (G115(®)) formulated with vitamins and minerals-an open-label study. Int J Environ Res Public Health 2021;18:6257.

[26] Chen YM, Wang IL, Zhou S, Tsai TY, Chiu YS, Chiu WC. Six weeks of Jilin ginseng root supplementation attenuates drop jump-related muscle injury markers in healthy female college students. Food Funct 2021;12:1458—68.

[27] Lee ES, Yang YJ, Lee JH, Yoon YS. Effect of high-dose ginsenoside complex (UG0712) supplementation on physical performance of healthy adults during a 12-week supervised exercise program: a randomized placebo-controlled clinical trial. J Ginseng Res 2018;42:192—8.

[28] Hitier S, Aran A, Pouteau E, Kim JY, Park JY, Kang HJ, Kim OY, Lee JH. Beneficial effects of Korean red ginseng on lymphocyte DNA damage, antioxidant enzyme activity, and LDL oxidation in healthy participants: a randomized, double-blind, placebo-controlled trial. Int J Environ Res Public Health 2012;11:47.

[29] Lee NH, Jung HC, Lee S. Red ginseng as an ergogenic aid: a systematic review of clinical trials. J Exerc Nutrition Biochem 2016;20:13—9.

[30] Reay JL, Scholey AB, Milne A, Fenwick J, Kennedy DO. Panax ginseng has no effect on indices of glucose regulation following acute or chronic ingestion in healthy volunteers. Br J Nutr 2009;101:1673—8.

[31] Ghavami A, Ziaei R, Foshati S, Hojati Kermani MA, Zare M, Amani R. Benefits and harms of ginseng supplementation on liver function? A systematic review and meta-analysis. Complement Ther Clin Pract 2020;39:101173.

[32] Irfan M, Kwak YS, Han CK, Hyun SH, Rhee MH. Adaptogenic effects of Panax ginseng on modulation of cardiovascular functions. J Ginseng Res 2020;44:538—43.

[33] Park SH, Chung S, Chung MY, Choi HK, Hwang JT, Park JH. Effects of Panax ginseng on hyperglycemia, hypertension, and hyperlipidemia: a systematic review and meta-analysis. J Ginseng Res 2022;46:188—205.

[34] Schilling JM, Roth DM, Patel HH. Caveolins in cardioprotection - translatability and mechanisms. Br J Pharmacol 2015;172:2114—25.

[35] Patel HH, Tsutsumi YM, Head BP, Niesman IR, Jennings M, Horikawa Y, Huang D, Moreno AL, Patel PM, Insel PA, et al. Mechanisms of cardiac protection from ischemia/reperfusion injury: a role for caveolae and caveolin-1. FASEB J 2007;21:1565—74.

[36] Jasmin JF, Rengo G, Lymperopoulos A, Gupta R, Eaton GJ, Quann K, Gonzales DM, Mercier I, Koch WJ, Lisanti MP. Caveolin-1 deficiency exacerbates cardiac dysfunction and reduces survival in mice with myocardial infarction. Am J Physiol Heart Circ Physiol 2011;300:H1274—81.

[37] Yun U-J, Lee J-H, Koo KH, Ye S-K, Kim S-Y, Lee C-H, Kim Y-N. Lipid raft modulation by Rp1 reverses multidrug resistance via inactivating MDR-1 and Src inhibition. Biochem Pharmacol 2013;85:1441—53.

[38] Fathil MF, Md Arshad MK, Gopinath SC, Hashim U, Adzhri R, Ayub RM, Ruslinda AR, Nuzaihan MNM, Azman AH, Zaki M, et al. Diagnostics on acute myocardial infarction: cardiac troponin biomarkers. Biosens Bioelectron 2015;70:209—20.

[39] Takahashi N, Ogita M, Suwa S, Nakao K, Ozaki Y, Kimura K, Ako J, Noguchi T, Yasuda S, Fujimoto K, et al. Prognostic impact of B-type natriuretic peptide on long-term clinical outcomes in patients with non-ST-segment elevation acute myocardial infarction without creatine kinase elevation. Int Heart J 2020;61:888—95.

[40] Chen X, Zhang X, Kubo H, Harris DM, Mills GD, Moyer J, Berretta R, Potts ST, Marsh JD, Houser SR. Ca^{2+} influx-induced sarcoplasmic reticulum Ca^{2+} overload causes mitochondrial-dependent apoptosis in ventricular myocytes. Circ Res 2005;97:1009—17.

[41] Zhong GG, Sun CW, Li YY, Qi H, Zhao CY, Jiang Y, Wang XM, Yang SJ, Li H. Calcium channel blockade and anti-free-radical actions of panaxadiol saponins Rb1, Rb2, Rb3, Rc, and Rd. Acta Pharmacologica Sinica 1995;16:255—60.

[42] Liu Z, Song L, Zhang P, Cao Z, Hao J, Tian Y, Luo A, Zhang P, Ma J. Ginsenoside Rb1 exerts antiarrhythmic effects by inhibiting I_{Na} and I_{CaL} in rabbit ventricular myocytes. Sci Rep 2019;9:20425.

[43] Lu C, Sun Z, Wang L. Inhibition of L-type Ca^{2+} current by ginsenoside Rd in rat ventricular myocytes. J Ginseng Res 2015;39:169—77.

[44] Zhang WJ, Li L, Zhao CY, Li X, Zhao M, Zhong GG. Effects of panaxadiol saponins monomer Rb1 on action potential and L-type calcium channel in ischemic cardiomyocytes. J Jilin Univ Med Edit 2007:978—81.

[45] Lee JH, Jeong SM, Kim JH, Lee BH, Yoon IS, Lee JH, Choi SH, Lee SM, Park YS, Lee JH, et al. Effects of ginsenosides and their metabolites on voltage-dependent Ca^{2+} channel subtypes. Mol Cells 2006;21:52—62.

[46] He F, Wu Q, Xu B, Wang X, Wu J, Huang L, Cheng J. Suppression of Stim1 reduced intracellular calcium concentration and attenuated hypoxia/reoxygenation induced apoptosis in H9C2 cells. Biosci Rep 2017;37.

[47] Tian W, Liu SY, Zhang M, Meng JR, Tang N, Feng YD, Sun Y, Gao YY, Zhou L, Cao W, et al. TRPC1 contributes to endotoxemia-induced myocardial dysfunction via mediating myocardial apoptosis and autophagy. Pharmacol Res 2022;181:106262.

[48] Chen Z, Wu J, Li S, Liu C, Ren Y. Inhibition of myocardial cell apoptosis is important mechanism for ginsenoside in the limitation of myocardial ischemia/reperfusion injury. Front Pharmacol 2022;13:806216.

[49] Brazer SC, Singh BB, Liu X, Swaim W, Ambudkar IS. Caveolin-1 contributes to assembly of store-operated Ca^{2+} influx channels by regulating plasma membrane localization of TRPC1. J Biol Chem 2003;278:27208—272015.

[50] Chaudhary KR, Cho WJ, Yang F, Samokhvalov V, El-Sikhry HE, Daniel EE, Seubert JM. Effect of ischemia reperfusion injury and epoxyeicosatrienoic acids on caveolin expression in mouse myocardium. J Cardiovasc Pharmacol 2013;61:258—63.

[51] Schilling JM, Dhanani M, Haushalter KJ, Howell SA, Verma R, Niesman IR, Zemljic-Harpf AE, Patel HH. Loss of caveolin-1 alters cardiac mitochondrial function and increases susceptibility to stress. J Mol Cell Cardiol 2017;112.165-165.

[52] Singh S, Mabalirajan U. Mitochondrial calcium in command of juggling myriads of cellular functions. Mitochondrion 2021;57:108—18.

[53] Shivshankar P, Halade GV, Calhoun C, Escobar GP, Mehr AJ, Jimenez F, Martinez C, Bhatnagar H, Mjaatvedt CH, Lindsey ML, et al. Caveolin-1 deletion exacerbates cardiac interstitial fibrosis by promoting M2 macrophage activation in mice after myocardial infarction. J Mol Cell Cardiol 2014;76:84—93.

[54] Wang Q, Fu W, Yu X, Xu H, Sui D, Wang Y. Ginsenoside Rg2 alleviates myocardial fibrosis by regulating TGF-β1/Smad signalling pathway. Pharm Biol 2021;59:106—13.

[55] Wang QW, Yu XF, Xu HL, Zhao XZ. Ginsenoside Re improves isoproterenol-induced myocardial fibrosis and heart failure in rats. Evid Based Complement Alternat Med 2019:3714508.

[56] Lai Q, Liu FM, Rao WL, Yuan GY, Fan ZY, Zhang L, et al. Aminoacylase-1 plays a key role in myocardial fibrosis and the therapeutic effects of 20(S)-ginsenoside Rg3 in mouse heart failure. Acta Pharmacol Sin 2022;43(8):2003—2015.

[57] Irfan M, Kim M, Rhee MH. Anti-platelet role of Korean ginseng and ginsenosides in cardiovascular diseases. J Ginseng Res 2020;44:24—32.

[58] Li W, Wu Y, Cai S, Tang C. Comparative effects of decreasing viscosity in different preparations of Chinese angelica root and ginseng. Zhong Yao Cai 2001;24:581—3.

[59] Chen IJ, Chang MY, Chiao SL, Chen JL, Yu CC, Yang SH, Liu JM, Hung CC, Yang RC, Chang HC, et al. Korean red ginseng improves blood pressure stability in patients with intradialytic hypotension. Evid Based Complement Alternat Med 2012;2012:595271.

[60] Yu Z, Han SY, Li HX, Tu PF. Effects of ginseng and safflower extractions on blood stream kinetics of heart in myocardial ischemia dogs. Chin J Basic Med Tradit Chin Med 2012;18:777—82.